CARBON 48 (2010) 3551–3558

available at www.sciencedirect.com

ScienceDirect

journal homepage: www.elsevier.com/locate/carbon

Increasing the electrical conductivity of carbon nanotube/polymer composites by using weak nanotube–polymer interactions

You Zeng [a,b], Pengfei Liu [b], Jinhong Du [a], Long Zhao [b], Pulickel M. Ajayan [c], Hui-Ming Cheng [a,*]

[a] Shenyang National Laboratory for Materials Science, Institute of Metal Research, Chinese Academy of Sciences, 72 Wenhua Road, Shenyang 110016, People's Republic of China

[b] School of Materials Science and Engineering, Shenyang Jianzhu University, 9 Hunnan East Road, Shenyang 110168, People's Republic of China

[c] Department of Mechanical Engineering and Materials Science, Rice University, 6100 Main Street, Houston, TX 77005, United States

ARTICLE INFO

Article history:
Received 2 November 2009
Accepted 25 May 2010
Available online 1 June 2010

ABSTRACT

A weak interaction between carbon nanotubes (CNTs) and polymers was found to reduce polymer-wrapping on CNT surface, decrease the contact resistance between CNTs, and increase the electrical conductivity of their composites. Thermodynamic properties such as surface energy of components, filler–polymer interactions, and wettability of carbon/polymer systems were analyzed. It was found that the graphitized CNTs filled polyoxymethylene (POM) system exhibits the weakest CNT–polymer interaction among all the investigated systems and a poor wettability. Consequently, the graphitized CNT/POM composites possess a high electrical conductivity and a low percolation threshold of 0.5 wt.% CNT loading, which is associated with the weak CNT–polymer interaction, low contact resistance between CNTs, good connectivity of CNT networks, and high crystallinity of POM in the composites. The results obtained imply that high-performance composites with optimal CNT-network structures can be designed and fabricated by fully considering the surface properties of components and CNT–polymer interactions.

1. Introduction

Interactions between carbon nanotubes (CNTs) and polymers play an important role in determining the ultimate performance of CNT/polymer composites [1–3]. A strong CNT–polymer interaction usually implies a strong interfacial bonding, a good load-transfer capability and a high mechanical strength of the composites, while functional properties of the composites greatly depend on the conductive structures of CNT networks and the CNT–polymer interactions. A small amount of CNT loading can remarkably increase the electrical conductivity of polymeric matrices due to the large aspect ratio (length to diameter ratio) and excellent electrical conductivity of CNTs [4–6]. There is a great potential for CNT/polymer composites to be commercially applied as electrical components in fields of electrical engineering, aerospace, transportation, and chemical industries.

Decreasing CNT loading amount by optimal structural design is generally effective for reducing cost and realizing commercial applications of CNT/polymer composites. A high crystallinity of polymeric matrices is theoretically helpful for fabricating a conductive network at a low CNT loading

* *Corresponding author:* Fax: +86 2423 903126.
E-mail address: cheng@imr.ac.cn (H.-M. Cheng).
0008-6223/$ - see front matter
doi:10.1016/j.carbon.2010.05.053

due to selective aggregation of CNTs at amorphous regions [7,8]. In fact, high CNT loading needed for obtaining the good conductivity of a composite is often observed even using highly crystalline polymers, such as high density polyethylene (HDPE) and polypropylene (PP), as matrices, for example, 2.5 wt.% CNT loading for CNT/HDPE composites [9], and 2 wt.% for CNT/PP composites [10]. The reason is that CNTs are easily wetted and wrapped by liquid polymers in manufacturing process due to the high surface energy of CNTs, resulting in a high contact resistance between the polymer-wrapped CNTs and a low electrical conductivity of the composites [11,12]. Recently some conductive polymers such as polyaniline, polypyrrole, and polythiophene, have been used to decrease the contact resistance between the wrapped CNTs, but there are still great challenges in processability and economy for these CNT-filled conductive polymer systems [13]. Since polymer-wrapping on CNT surface leads to a drastic increase in contact resistance between the wrapped CNTs [14], decreasing the surface energy of CNTs and weakening the CNT–polymer interaction would be helpful for reducing the polymer-wrapping around CNTs, and increasing the electrical conductivity of CNT/polymer composites.

The objective of this research is to fabricate CNT/polymer composites with a high electrical conductivity using a methodology of weak CNT–polymer interactions. Firstly, thermodynamic properties of several carbon/polymer systems, such as the surface energy of components, CNT–polymer interactions and wettability, were analyzed on the basis of surface physics and chemistry. The results show that graphitized CNTs (g-CNTs) filled polyoxymethylene (POM) systems exhibit the weakest interaction among all the investigated systems and a poor wettability. Secondly, crystallization kinetics of the g-CNT/POM composites was investigated for elucidating the effects of weak CNT–POM interaction on the formation of CNT networks in POM matrix. Finally, the microstructure and electrical conductivity of the composites were investigated. As we anticipated, the g-CNT/POM composites exhibit a high electrical conductivity with a low percolation threshold of 0.5 wt.% CNTs, which is closely associated with the weak CNT–polymer interaction, good connectivity of CNT networks, and high crystallinity of the matrix. The results obtained imply that high-performance composites with optimal CNT-network structures can be designed and fabricated by fully considering the surface properties of components and CNT–polymer interactions.

2. Experimental

2.1. Graphitization of carbon nanotubes

Pristine multi-walled CNTs, produced by using a chemical vapor deposition method and supplied from Shenyang Gina New Material Co., Ltd., were graphitized at 2600 °C in high-purity argon atmosphere for 45 min in order to remove structural defects and decrease surface energy of the CNTs [15]. Microstructures of the graphitized CNTs (g-CNTs) were observed by using a scanning electron microscopy (SEM) and transmission electron microcopy (TEM). The CNTs have a large aspect ratio over 500 and an average diameter of 50–100 nm.

2.2. Crystallization kinetics of CNT/polymer composites

Non-isothermal crystallization behaviors of CNT/polymer composites were investigated by using a differential scanning calorimetry (DSC) technique for evaluating the effects of CNT–polymer interaction on crystallization kinetics of the composites. Polyoxymethylene (POM, Delrin 390PM supplied from DuPont Co.) and the g-CNT/POM composites with different CNT loading amounts of 0.5, 1, 2, 4, and 6 wt.%, were heated up to 190 °C in nitrogen atmosphere and kept for 5 min to eliminate previous thermal history, and then cooled down at constant rates of 2.5, 5, 10, and 20 °C/min. Non-isothermal crystallization kinetics of the g-CNT/POM composites was further analyzed by means of the Avrami, Ozawa and combined Avrami–Ozawa models.

2.3. Fabrication and microstructures of CNT/polymer composites

The g-CNT/POM composites were prepared by using conventional melt-mixing and hot pressing techniques. POM pellets were molten at 190 °C in an internal two-roller mixer at a rotation speed of 30 rpm, and then the weighed g-CNTs were added into and well mixed with the molten POM for 10 min at 190 °C at 90 rpm. Subsequently the g-CNT/POM blends were transferred into a hot pressing machine and molded into g-CNT/POM composite sheets of 1 mm in thickness under a pressure of 10 MPa at 190 °C. Microstructures of the composites were observed by means of SEM, and degrees of crystallization (X_c) of the composites were measured by using a DSC instrument in air at a constant heating rate of 10 °C/min.

2.4. Electrical conductivity of CNT/polymer composites

The g-CNT/POM composite sheets were tailored into square specimens of 10 mm × 10 mm, and upper and lower surfaces of the specimens were coated with conducting silver paint to ensure an intimate contact between the specimen surfaces and electrodes. Electrical resistance (R_v) of the composites was measured by using a digital multimeter for R_v less than 10^7 Ω or using a high-resistance meter for R_v over 10^7 Ω alternatively, and the electrical conductivity (σ) of the composites was calculated according to the following formula:

$$\sigma = t/(R_v \times A) \quad (1)$$

where t and A are thickness of the specimens and effective area of the measuring electrodes, respectively.

3. Results and discussion

3.1. Interactions between fillers and polymers

Filler–polymer interactions in carbon/polymer composites largely depend on the surface properties of both components. The surface energy (γ) of components in several carbon/polymer systems is listed in Table 1 [16–21]. Both carbon black (CB) and pristine CNTs show much higher surface energy than molten polymers such as HDPE, PP, and POM, implying that there is a tendency for low surface-energy polymers to spontaneously aggregate on filler surfaces for minimizing total

Table 1 – Surface energy of components in the carbon/polymer systems investigated.

Components	Dispersion tension γ^d (mJ/m^2)	Polarity tension γ^p (mJ/m^2)	Polarity χ^p	Surface energy γ (mJ/m^2)[A]
Carbon black[B]	94.5	3.6	0.1	98.1
Pristine CNTs[C]	26.9	18.4	0.4	45.3
g-CNTs[D]	21.8	1.8	0.1	23.6
HDPE (200 °C)[E]	25.4	0.0	0.0	25.4
PP (200 °C)[E]	19.3	0.0	0.0	19.3
POM (190 °C)[F]	14.3	6.7	0.3	21.0

[A] Surface energy (γ) consists of dispersion tension (γ^d) and polarity tension (γ^p).
[B] Refs. [16] and [17].
[C] Ref. [18].
[D] Surface energy of the g-CNTs was assumed to approach that of graphite powders (Ref. [19]) on account of similar graphitic microstructures between the g-CNTs and the graphite powders.
[E] Ref. [20].
[F] Ref. [21].

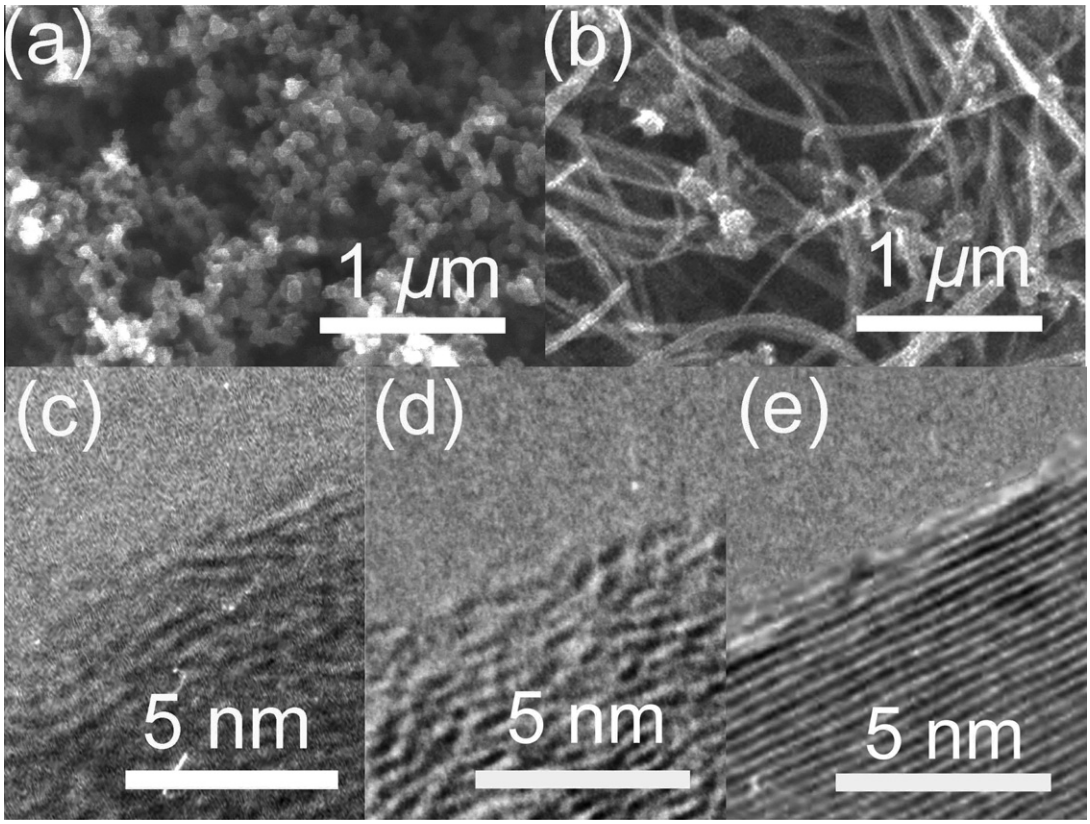

Fig. 1 – SEM images of: (a) CB and (b) CNTs. HRTEM images of: (c) CB, (d) pristine CNTs and (e) g-CNTs, revealing the g-CNTs have the most integrated graphitic planes.

energy of the systems. However, wrapping of insulating polymers around conductive fillers can greatly increase contact resistance between the fillers, and thus result in a low electrical conductivity [14]. Therefore, decreasing the surface energy of conductive fillers may be an effective method for reducing the polymer-wrapping around fillers and increasing the electrical conductivity of the composites.

Compared with CB and pristine CNTs, the g-CNTs exhibit a lower γ value of 23.6 mJ/m^2 in Table 1 and a more integrated microstructure shown in Fig. 1. It is necessary to point out that the accurate γ measurement of nanoparticles is extremely complicated because γ value strongly depends on many factors such as sample sizes, microstructures, surface functional groups, and even measuring methods [22,23]. In spite of the complexity of measurements, there are still some widely-accepted viewpoints on the surface energy of carbon materials: firstly, graphitization treatment can effectively remove polar functional groups from sample surfaces and result in a low value of polarity tension (γ^p) [24]; secondly, graphitic planes generally exhibit a lower γ value than other

Table 2 – Interactions and wettability of the carbon/polymer systems investigated.[a]

Components	Work of adhesion W_a (mJ/m^2)			Spreading coefficient S (mJ/m^2)		
	HDPE	PP	POM	HDPE	PP	POM
Carbon black	80.1	64.1	59.0	29.3	25.5	17.0
Pristine CNTs	52.2	44.9	57.0	1.4	6.3	15.0
g-CNTs	46.9	40.9	40.2	−3.9	2.3	−1.8

[a] Interactions and wettability are represented by work of adhesion (W_a) and spreading coefficient (S), respectively; the data were calculated according to the thermodynamic equations in Ref. [27].

sites such as amorphous carbon, crystallite edges, and cavities [25]; thirdly, integrated microstructures and large sizes of crystalline grains also result in a low γ value [26]. In our work, the g-CNTs have few surface functional groups, integrated graphitic planes and large crystalline gains [15], and thus exhibit a low value of surface energy as shown in Table 1. Such a low γ value of the g-CNTs would have considerable influences on CNT–polymer interactions and polymer-wrapping around CNTs.

Table 2 lists the interactions and wettability of the carbon/polymer systems investigated in terms of the work of adhesion (W_a) and spreading coefficient (S). The values of W_a and S were calculated according to the thermodynamic Eqs. (2) and (3) [27]:

$$W_a = \gamma_{gs} + \gamma_{gl} - \gamma_{sl} = \frac{4\gamma_s^d\gamma_l^d}{\gamma_s^d + \gamma_l^d} + \frac{4\gamma_s^p\gamma_l^p}{\gamma_s^p + \gamma_l^p} \quad (2)$$

$$S = \gamma_{gs} - \gamma_{sl} - \gamma_{gl} = W_a - 2\gamma_{gl} \quad (3)$$

where the subscript g, s and l stand for gas, solid and liquid phases, respectively; a criterion for liquid spontaneously wetting solid is that the S value is less than zero. It is worth pointing out that the values of W_a and S are only inversely proportional to the values of γ_s^d *and* γ_s^p once the polymeric matrix is fixed (the values of γ_l^d, γ_l^p and γ_{gl} are constant). As shown in Table 2, the g-CNT/polymer systems exhibit much lower values of W_a and S than other carbon/polymer systems, implying a weak CNT–polymer interaction and a poor wettability, which is closely associated with the low surface energy of the g-CNTs. Furthermore, the g-CNT/POM system exhibits the weakest CNT–polymer interaction (a W_a value as low as 40.2 mJ/m^2) among all the investigated systems, and their S value is only −1.8 mJ/m^2 and less than zero, implying that the g-CNTs cannot be spontaneously wetted by the molten POM in the melt-mixing process. The weak interaction and poor wettability of the g-CNT/POM system may play an important role in reducing polymer-wrapping around CNTs, influencing crystallization behaviors and microstructures of the composites, decreasing contact resistance between CNTs, and increasing the electrical conductivity of CNT/polymer composites.

3.2. *Crystallization kinetics of CNT/polymer composites*

Effects of the g-CNTs on crystallization behaviors of the g-CNT/POM composites were investigated, and the kinetic parameters of crystallization rates and nucleation mechanism were described by means of the Avrami, Ozawa and combined Avrami–Ozawa models (see the Supplementary material) [28,29]. Fig. 2 shows crystallization rates of the g-CNT/POM composites at different CNT loading amounts. Compared with neat POM, the g-CNT/POM composites exhibit a lower crystallization rate, e.g., longer crystallization half-time ($t_{1/2}$), smaller growth rate constant (Z_c), and higher kinetic parameter (F_T). The slow crystallization process of the g-CNT/POM composites is closely associated with the weak CNT–polymer interactions. It is worth mentioning that CNTs usually play a role of nucleating agents in accelerating crystallization in various CNT/polymer systems [30,31]; however, in our work, the g-CNTs did not induce nucleation and increase crystallization rate of POM as a nucleating agent did. The reason is that the g-CNTs have a low γ value and a poor wettability, and it is difficult for the g-CNTs to induce aggregation of polymeric chains on their low-energy surfaces; on the other hand, the presence of g-CNTs in the molten POM can hinder rearrangement of polymeric chains during crystallization and thus result in a decrease in the crystallization rate of the composites [32]. Therefore, the slow crystallization rate of g-CNT/POM composites is closely associated with the low surface energy of g-CNTs and the weak CNT–polymer interaction.

The g-CNT/POM composite with 1 wt.% CNT loading exhibits the lowest crystallization rate, the maximum values of $t_{1/2}$ and F_T, and the minimum value of Z_c among all the samples; such a dependence of crystallization rate on CNT loading is closely related with the CNT–polymer interaction during crystallization. Fig. 2d illustrates the influences of CNTs on crystallization behaviors of g-CNT/POM composites at a low CNT loading. The crystallization process of g-CNT/POM composites is a gradual growth process of POM spherulites consisting of flat ribbon-like folded-chain lamellar crystals (so-called fibrils), which have a thickness of ca. 10–50 nm, a width of ca. 50 nm, and a large aspect ratio over 100 [33,34]. It is interesting that there is a morphological similarity between the CNTs and the fibrils due to their large aspect ratios and comparable diameters, implying a similarity in movement ability between the CNTs and the fibrils during crystallization. In the case of low CNT loading, the growing fibrils can push individually dispersed CNTs to move when the fibrils collide with CNTs during the spherulite growth. The resulting motion of rigid CNTs greatly disturbs the ordered arrangement of polymeric chains, just as a rotating stirrer does during crystallization [34], and thus results in slow crystallization of the composites at low CNT loading. On the contrary, when the CNT loading is over 2 wt.%, a connecting CNT network has been formed throughout the molten matrix even

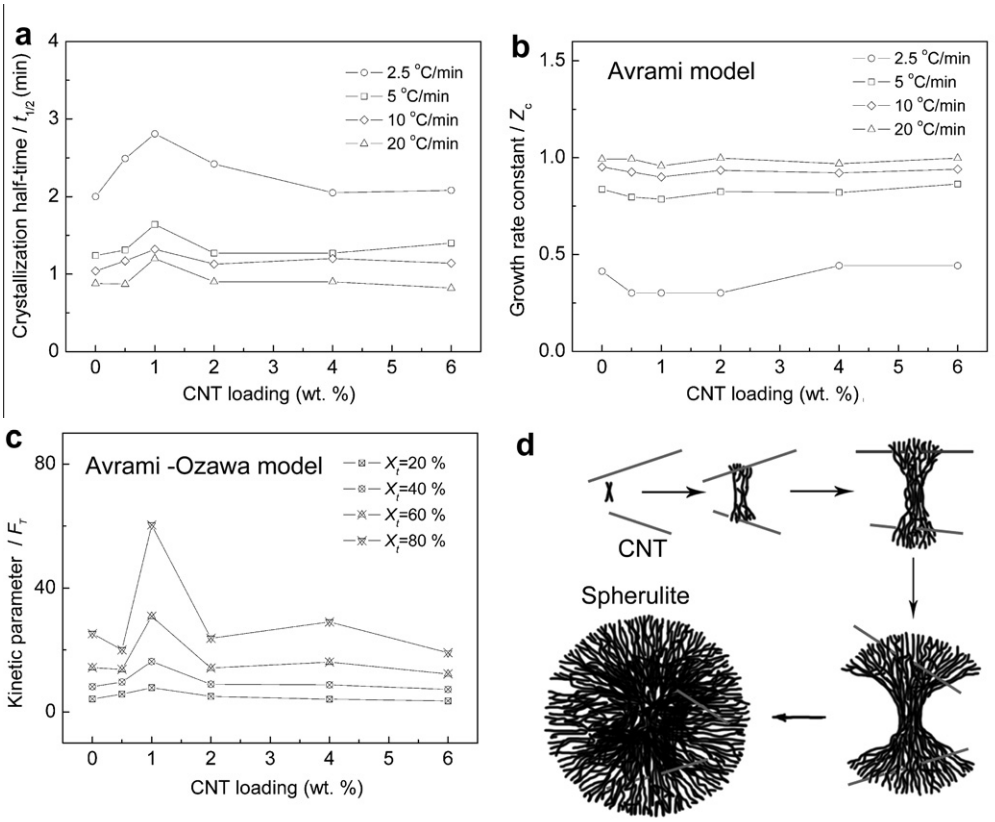

Fig. 2 – Effects of g-CNTs on crystallization rates represented in terms of: (a) crystallization half-time $t_{1/2}$, (b) growth rate constant Z_c, and (c) kinetic parameter F_T. (d) A schematic of the interaction between CNTs and POM fibrils during crystallization.

before crystallization. The growing fibrils hardly cause motions of the stable CNT network during crystallization, and they continuously diverge and grow in their original growth manners [34]. As a result, the g-CNT/POM composites at high CNT loading maintain a crystallization rate as high as the neat POM. Therefore, the influences of g-CNTs on the crystallization kinetics of g-CNT/POM composites are closely associated with the CNT–polymer interactions during crystallization. It is notable that further investigations based on the CNT-fibril similarity in morphology and movement ability would perhaps reveal significant synergistic effects between CNTs and polymers in the crystallization process of CNT/polymer composites.

3.3. *Microstructures and crystallinity of CNT/polymer composites*

The g-CNT/POM composites exhibit highly crystalline structures and high degrees of crystallization in Fig. 3. Firstly, large POM spherulites of ca. 30 μm in diameter can be clearly observed on fracture surfaces of the composites, and the fibrils show a similar morphology and comparable diameters with the CNTs used as mentioned above. Secondly, smooth surfaces of g-CNTs pulled out of POM matrix reveal a weak interfacial bonding between the g-CNTs and the POM matrix, resulting from the weak CNT–polymer interactions and the poor wettability of the g-CNT/POM system. The unwrapped CNTs are beneficial to decreasing contact resistance between CNTs and increasing the electrical conductivity of the composites [35]. Moreover, it is interesting to note that the CNTs lie between POM fibrils, penetrating through POM spherulites and forming a CNT–spherulite interpenetrating network in the composites as shown in Fig. 3d. Such an interpenetrating structure is helpful for increasing electrical conductivity and thermal stability of CNT/polymer composites [8]. In Fig. 3e, all the g-CNT/POM composites with different CNT loading amounts exhibit the degrees of crystallization over 60%, nearly as high as the neat POM in spite of a little decrease in the crystallization rate as mentioned above, which is mainly due to the weak CNT–POM interactions and the high crystallinity of POM. Such a high crystallinity of the g-CNT/POM composites is helpful for increasing electrical conductivity of the composites at a low CNT loading due to the selective aggregation of CNTs in amorphous regions of polymeric matrices.

3.4. *Electrical conductivity of CNT/polymer composites*

The g-CNT/POM composites exhibit a high electrical conductivity (σ) in Fig. 4, and their percolation threshold, which is the CNT loading needed for obtaining a reasonable conductivity of the composites, is as low as 0.5 wt.%. Theoretical analyses were performed according to the scaling law [36]:

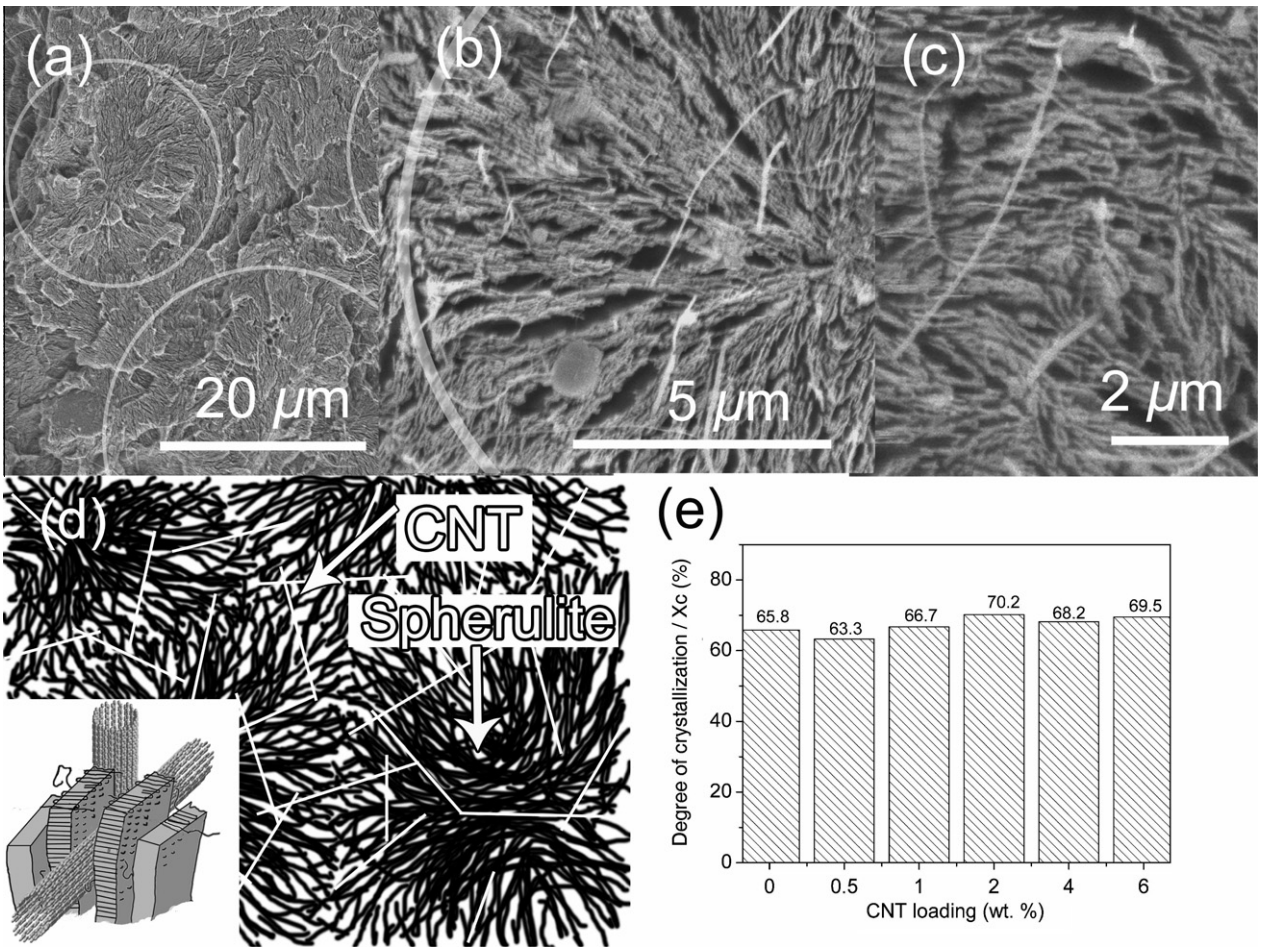

Fig. 3 – SEM images of g-CNT/POM composites with 1 wt.% CNT loading amount (a–c) at different magnifications. (d) A structural model illustrating that the g-CNTs unwrapped by insulating polymer lie between spherulite fibrils and form a CNT–spherulite interpenetrating network. (e) Degree of crystallization of the g-CNT/POM composites.

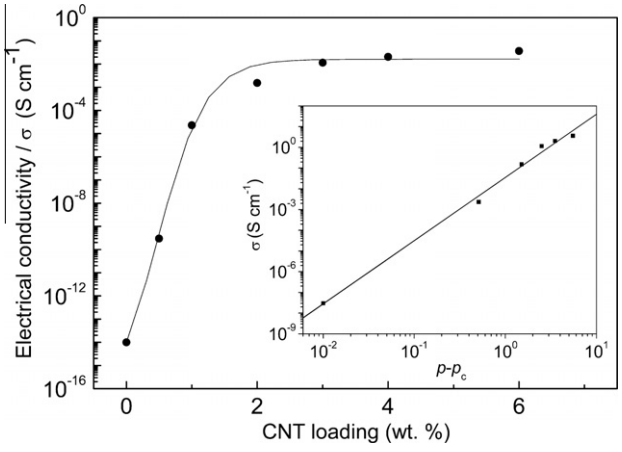

Fig. 4 – Electrical conductivity (σ) of g-CNT/POM composites as a function of CNT loading.

$$\sigma = (p - p_c)^t \quad (4)$$

where p and p_c are CNT loading amount (mass fraction) and percolation threshold, respectively; t is a scaling exponent. The inset in Fig. 4 reveals a good fit of the experimentally measured conductivity to the scaling law, indicating that the electrical conductivity of the g-CNT/POM composites can be well explained in terms of the percolation theory [36]. On the other hand, the exponent t is expected to depend on sample dimensionality with calculated values of $t \sim 1.33$ and $t \sim 2.0$ for thin-film and bulk samples, respectively [37]. In our work, the t value of the g-CNT/POM composites with a 1 mm thickness is as low as 1.38, much less than the value of 2.0 theoretically anticipated for a three-dimensional bulk sample; such a low t value implies an enhancement in electron transport of the composites, resulting from effective overlapping and low contact resistance between the unwrapped g-CNTs [6,38]. Therefore, the high electrical conductivity of g-CNT/POM composites is closely associated with the weak CNT–polymer interaction, low contact resistance between the g-CNTs, and high crystallinity of POM. Although the electrical conductivity of CNT/polymer composites can be influenced by other factors such as diameter of CNTs, intrinsic conductivity of CNTs, and effectiveness of conductive networks, the weak CNT–polymer interaction described in this study definitely plays an extremely important role in reducing polymer-wrapping around CNTs, influencing the crystallization behaviors, fabricating the CNT network in

matrices, and consequently increasing the electrical conductivity of CNT/polymer composites.

4. Conclusion

CNT/polymer composites with a high electrical conductivity were designed and fabricated using the methodology of weak CNT–polymer interactions. The thermodynamic properties such as surface energy, wettability, and filler–polymer interaction, in various carbon/polymer systems were calculated and analyzed for reducing polymer-wrapping around CNTs and decreasing the contact resistance between CNTs. The analysis reveals that g-CNT/POM systems have the weakest CNT–polymer interaction among the investigated systems and exhibit a poor wettability. Furthermore, the crystallization kinetics, microstructures, and electrical conductivity of the g-CNT/POM composites were investigated for elucidating the effects of weak CNT–polymer interactions. The g-CNT/POM composites exhibit a high electrical conductivity and a low percolation threshold of 0.5 wt.%, which is closely associated with the weak CNT–polymer interaction, low contact resistance between CNTs, and high crystallinity of the composites. The weak CNT–polymer interaction has remarkable influences on the wettability, crystallization behaviors, fabrication of CNT networks in matrices, and enhancement of electrical conductivity of the composites. Therefore, high-performance composites with an optimal conductive network can be deliberately designed and fabricated by fully considering the surface properties of components, filler–polymer interactions, and structures of the conductive network in matrices.

Acknowledgements

The authors thank Dr. F. Li and Dr. X. Tong for the measurements of crystallization kinetics. Financial supports from NSFC (Nos. 90606008 and 50921004), MOST (No. 2006CB932703), and LNED (No. 2008589) are acknowledged.

Appendix A. Supplementary data

Supplementary data and analyses on crystallization kinetics of the graphitized CNT/POM composites can be found in the online version, at doi:10.1016/j.carbon.2010.05.053.

REFERENCES

[1] Ajayan PM, Tour JM. Nanotube composites. Nature 2007;447(7148):1066–8.
[2] Wei CY. Radius and chirality dependent conformation of polymer molecule at nanotube interface. Nano Lett 2006;6(8):1627–31.
[3] Czerw R, Guo ZX, Ajayan PM, Sun YP, Carroll DL. Organization of polymers onto carbon nanotubes: a route to nanoscale assembly. Nano Lett 2001;1(8):423–7.
[4] McNally T, Pötschke P, Halley P, Murphy M, Martin D, Bell SEJ, et al. Polyethylene multiwalled carbon nanotube composites. Polymer 2005;46(19):8222–32.
[5] Breuer O, Sundararaj U. Big returns from small fibers: a review of polymer/carbon nanotube composites. Polym Comp 2004;25(6):630–45.
[6] Sandler JKW, Kirk JE, Kinloch IA, Shaffer MSP, Windle AH. Ultra-low electrical percolation threshold in carbon–nanotube–epoxy composites. Polymer 2003;44(19):5893–9.
[7] Moniruzzaman M, Winey KI. Polymer nanocomposites containing carbon nanotubes. Macromolecules 2006;39(16):5194–205.
[8] He XJ, Du JH, Ying Z, Cheng HM, He XJ. Positive temperature coefficient effect in multiwalled carbon nanotube/high-density polyethylene composites. Appl Phys Lett 2005;86(6):062112-1–3.
[9] Valentino O, Sarno M, Rainone NG, Nobile MR, Ciambelli P, Neitzert HC, et al. Influence of the polymer structure and nanotube concentration on the conductivity and rheological properties of polyethylene/CNT composites. Phys E 2008;40(7):2440–5.
[10] Lee SH, Cho E, Jeon SH, Youn JR. Rheological and electrical properties of polypropylene composites containing functionalized multi-walled carbon nanotubes and compatibilizers. Carbon 2007;45(14):2810–22.
[11] Dalmas F, Dendievel R, Chazeau L, Cavaille JY, Gauthier C. Carbon nanotube-filled polymer of electrical conductivity in composites. Numerical simulation three-dimensional entangled fibrous networks. Acta Mater 2006;54(11):2923–31.
[12] Sun XX, Song M. Highly conductive carbon nanotube/polymer nanocomposites achievable? Macromol Theor Simul 2009;18(3):155–61.
[13] Hatchett DW, Josowicz M. Composites of intrinsically conducting polymers as sensing nanomaterials. Chem Rev 2008;108(2):746–69.
[14] Li CY, Thostenson ET, Chou TW. Dominant role of tunneling resistance in the electrical conductivity of carbon nanotube-based composites. Appl Phys Lett 2007;91(22):223114-1–3.
[15] Zeng Y, Ying Z, Du JH, Cheng HM. Effects of carbon nanotubes on processing stability of polyoxymethylene in melt-mixing process. J Phys Chem C 2007;111(37):13945–50.
[16] Wu GZ, Asai S, Sumita M, Yui H. Entropy penalty-induced self-assembly in carbon black or carbon fiber filled polymer blends. Macromolecules 2002;35(3):945–51.
[17] Koysuren O, Yesil S, Bayram G. Effect of surface treatment on electrical conductivity of carbon black filled conductive polymer composites. J Appl Polym Sci 2007;104(5):3427–33.
[18] Nuriel S, Liu L, Barber AH, Wagner HD. Direct measurement of multiwall nanotube surface tension. Chem Phys Lett 2005;404(4–6):263–6.
[19] Yu Y, Shi H. On humid and surface free energy properties of powder-graphite. J Saf Env 2007;7(1):60–1.
[20] Brandrup J, Immergut EH, Grulke EA. Polymer handbook. 4th ed. New York: John Wiley and Sons, Inc.; 1999. p. VI 524–35.
[21] Tajima Y. Structure of polyacetal polymer blends filled with carbon black. Kobunshi Ronbunshu 2005;62(3):104–8.
[22] Schröder A, Klüppel M, Schuster RH. Characterisation of surface activity of carbon black and its relation to polymer–filler interaction. Macromol Mater Eng 2007;292(8):885–916.
[23] Fu Q, Weinberg G, Su DS. Selective filling of carbon nanotubes with metals by selective washing. N Carbon Mater 2008;23(1):17–20.
[24] Kim YA, Hayashi T, Osawa K, Dresselhaus MS, Endo M. Annealing effect on disordered multi-wall carbon nanotubes. Chem Phys Lett 2003;380(3–4):319–24.
[25] Schröder A, Klüppel M, Schuster RH, Heidberg J. Surface energy distribution of carbon black measured by static gas adsorption. Carbon 2002;40(2):207–10.
[26] Zhang SY, Wei LM, Gu HC, Zhu YN. Relationship research between nano-structure of carbon black surface and

dispersive free energy of carbon black. J Mater Sci Eng 2006;24(3):337–40.
[27] Butt H, Graf K, Kappl M. Physics and chemistry of interfaces. Weinheim: Wiley-VCH Verlag GmbH and Co.; 2003. p. 131–3.
[28] Mitchell CA, Krishnamoorti R. Non-isothermal crystallization of in situ polymerized poly(epsilon-caprolactone) functionalized-SWNT nanocomposites. Polymer 2005;46(20):8796–804.
[29] Kim JY, Park HS, Kim SH. Unique nucleation of multi-walled carbon nanotube and poly(ethylene 2,6-naphthalate) nanocomposites during non-isothermal crystallization. Polymer 2006;47(4):1379–89.
[30] Li LY, Li CY, Ni CY. Polymer crystallization-driven, periodic patterning on carbon nanotubes. J Am Chem Soc 2006;128(5):1692–9.
[31] Ryan KP, Lipson SM, Drury A, Cadek M, Ruether M, O'Flaherty SM, et al. Carbon-nanotube nucleated crystallinity in a conjugated polymer based composite. Chem Phys Lett 2004;391(4–6):329–33.
[32] Jog JP. Crystallisation in polymer nanocomposites. Mater Sci Technol 2006;22(7):797–806.
[33] Bower DI. An introduction to polymer physics. Cambridge: Cambridge University Press; 2002. p. 133–7.
[34] Reiter G, Strobl GR. Progress in understanding of polymer crystallization. Berlin, Heidelberg: Springer; 2007. p. 3–15.
[35] Allaoui A, Hoa SV, Evesque P, Bai JB. Electronic transport in carbon nanotube tangles under compression: the role of contact resistance. Scripta Mater 2009;61(6):628–31.
[36] Stauffer D, Aharony A. Introduction to percolation theory. 2nd ed. Philadelphia: Taylor and Francis; 2003. p. 34–40.
[37] Kilbride BE, Coleman JN, Fraysse J, Fournet P, Cadek M, Drury A, et al. Experimental observation of scaling laws for alternating current and direct current conductivity in polymer–carbon nanotube composite thin films. J Appl Phys 2002;92(7):4024–30.
[38] Reghu M, Yoon CO, Yang CY, Moses D, Smith P, Heeger AJ, et al. Transport in polyaniline networks near the percolation threshold. Phys Rev B 1994;50(19):13931–41.